In vivo microscopy reveals the impact of *Pseudomonas aeruginosa* social interactions on host colonization

Chiara Rezzoagli[1,2*], Elisa T. Granato[3], Rolf Kümmerli[1,2*]

[1]Department of Plant and Microbial Biology, University of Zurich, Zurich, Switzerland

[2]Department of Quantitative Biomedicine, University of Zurich, Zurich, Switzerland

[3]Department of Zoology, University of Oxford, Oxford, United Kingdom

Running title: Bacterial social dynamics and host colonization

* Corresponding authors:

Chiara Rezzoagli or Rolf Kümmerli, Department of Quantitative Biomedicine, University of Zurich, Winterthurerstrasse 190, 8057 Zurich, Switzerland.

Email: chiara.rezzoagli@uzh.ch (CR), rolf.kuemmerli@uzh.ch (RK).

Phone: +41 44 635 48 01.

Conflict of interest: The authors declare no conflict of interest.

Abstract

Pathogenic bacteria engage in social interactions to colonize hosts, which include quorum-sensing-mediated communication and the secretion of virulence factors that can be shared as “public goods” between individuals. While *in-vitro* studies demonstrated that cooperative individuals can be displaced by “cheating” mutants freeriding on social acts, we know less about social interactions in infections. Here, we developed a live imaging system to track virulence factor expression and social strain interactions in the human pathogen *Pseudomonas aeruginosa* colonizing the gut of *Caenorhabditis elegans*. We found that shareable siderophores and quorum-sensing systems are expressed during infections, affect host gut colonization, and benefit non-producers. However, non-producers were unable to cheat and outcompete producers. Our results indicate that the limited success of cheats is due to a combination of the down-regulation of virulence factors over the course of the infection, the fact that each virulence factor examined contributed to but was not essential for host colonization, and the potential for negative-frequency dependent selection. Our findings shed new light on bacterial social interactions in infections and reveal potential limits of therapeutic approaches that aim to capitalize on social dynamics between strains for infection control.

Introduction

During infections, pathogenic bacteria secrete a wide range of extracellular virulence factors to colonize and grow inside the host [1, 2]. Secreted molecules include siderophores for iron scavenging, signaling molecules for quorum sensing (QS), toxins to attack host cells, and matrix compounds for biofilm formation [3–6]. *In-vitro* studies have shown that extracellular virulence factors can be shared as "public goods" between cells, and thereby benefit individuals other than the producing cell [7–9]. There has been enormous interest in understanding how this form of bacterial cooperation can be evolutionarily stable since secreted public goods can be exploited by non-cooperative mutants called "cheats", which do not engage in cooperation yet still benefit from the molecules produced by others [10–12].

There is increasing evidence that social interactions and cooperator-cheat dynamics might also matter within hosts [9, 13, 14]. For instance, in controlled infection experiments engineered non-producers, deficient for the production of specific virulence factors, could outcompete producers and thereby reduce virulence [15–19], but in other cases the success of non-producers was compromised [20, 21]. Other studies have followed chronic human infections within patients over time and reported that virulence-factor-negative mutants emerge and spread, with the mutational patterns suggesting cooperator-cheat dynamics [7, 22, 23]. These findings spurred ideas of how social interactions within hosts could be manipulated for therapeutic purposes [14, 24, 25]. Suggested approaches include: inducing cooperator-cheat dynamics to steer infections towards lower virulence [7, 26]; introducing less virulent strains with

63 medically beneficial alleles into established infections [24]; and targeting
64 secreted virulence factors to control infections and constrain the evolution of
65 resistance [25, 27–31].
66
67 However, all these approaches explicitly rely on the assumption that the social
68 traits of interest are: (i) expressed inside hosts; (ii) important for host
69 colonization; (iii) exploitable; and (iv) induce cooperator-cheat dynamics as
70 observed *in vitro* [9] – assumptions that have not yet been tested in real time
71 inside living hosts. Here, we explicitly test the importance of bacterial social
72 interactions within hosts by using *in-vivo* fluorescence microscopy to monitor
73 bacterial virulence factor production, host colonization and strain interactions,
74 using the opportunistic pathogen *Pseudomonas aeruginosa* and its nematode
75 model host *Caenorhabditis elegans* [32–34].
76
77 *C. elegans* naturally preys on bacteria [35]. While most bacteria are killed
78 during ingestion, a small fraction of cells survives [36], which can, in the case
79 of pathogenic bacteria, establish an infection in the gut [37]. *P. aeruginosa*
80 deploys an arsenal of virulence factors that facilitate successful host
81 colonization [38]. For example, the two siderophores pyoverdine and pyochelin
82 scavenge host-bound iron during acute infections to enable pathogen growth
83 [6, 39–41]. *P. aeruginosa* further secretes the protease elastase, the toxin
84 pyocyanin, and rhamnolipid biosurfactants to attack host tissue [7, 42, 43].
85 Production of these latter virulence factors only occurs at high cell densities
86 and is controlled by the Las and the Rhl QS-systems [44]. Because both QS-

regulated virulence factors and siderophores were shown to be involved in *C. elegans* killing [37, 45–48], we used them as focal traits for our study.

To tackle our questions, we first conducted experiments with fluorescently tagged *P. aeruginosa* bacteria (PAO1) to follow infection dynamics, from the first uptake through feeding up to a progressed state of gut infection. We then constructed promoter-reporter fusions for genes involved in the synthesis of the two siderophores (pyoverdine and pyochelin) and the two QS-regulators (LasR and RhlR) to track *in vivo* virulence factor gene expression during host colonization. Subsequently, we used mutant strains deficient for virulence factors to determine whether they show compromised colonization abilities. Finally, we followed mixed infections of wildtype and mutants over time to determine the extent of strain co-localization in the gut, and to test whether secreted virulence factors are indeed exploitable by non-producers in the host.

Material and methods

Strain and bacterial growth conditions

Bacterial strains, primers and plasmids used in this study are listed in the Supplementary Tables S1-S3. Details on strain construction are given in the Supplementary Methods. For all experiments, overnight cultures were grown in 8 ml Lysogeny broth (LB) in 50 ml tubes, incubated at 37°C, 220 rpm for 18 hours, washed with 0.8% NaCl solution and adjusted them to OD_{600} = 1. Nematode Growth Media (NGM) plates [0.25% Peptone, 50 mM NaCl, 25mM [PO_4^-], 5 µg/ml Cholesterol, 1mM $CaCl_2$, 1mM $MgSO_4$ supplemented with 1.5% agar, 6 cm diameter] were seeded with 50 µl of bacterial culture and

incubated at 25°C for 24 hours. All *P. aeruginosa* strains used in this study showed equal growth on NGM exposure plates (Supplementary Figure S1). Peptone was purchased from BD Biosciences, Switzerland, all other chemicals from Sigma Aldrich, Switzerland.

Nematode culture

We used the temperature-sensitive, reproductively sterile *C. elegans* strain JK509 (*glp-1*(*q231*) III). This strain reproduces at 16°C, but does not develop gonads and is therefore sterile at 25°C. Worms were maintained fertile at 16°C on High Growth Media (HGM) agar plates (2% Peptone, 50 mM NaCl, 25mM $[PO_4^-]$, 20 µg/ml Cholesterol, 1mM $CaCl_2$, 1mM $MgSO_4$) seeded with the standard food source *E. coli* strain OP50 [49]. For age synchronization, plates were washed with sterile distilled water and adult worms were killed with hypochlorite-sodium hydroxide solution to isolate eggs [49]. Eggs were placed in M9 buffer (20 mM KH_2PO_4, 40 mM Na_2HPO_4, 80 mM NaCl, 1 mM $MgSO_4$) and incubated at 16°C for 16-18 hours to hatch. Then, L1 larvae were transferred to OP50-seeded HGM plates and incubated at 25°C for 28 hours to reach L4 developmental stage. Worms and OP50 bacteria were provided by the Caenorhabditis Genetic Center (CGC), which is supported by the National Institutes of Health - Office of Research Infrastructure Programs (P40 OD010440).

***C. elegans* infection protocol**

Synchronized L4 worms were washed from HGM plates with M9 buffer + 50 µg/ml kanamycin (M9-Kan), and washed three times with M9-Kan for worm

surface-disinfection. Viable worms were further separated from any debris by sucrose flotation [50] and rinsed three time in M9 buffer to remove sucrose. The worm handling protocol for the main experiments is depicted in Figure 1A. Specifically, approximately 200 worms were moved to seeded NGM plates and incubated for 24 hours at 25°C. After this period of exposure to pathogens, infected worms were extensively washed with M9 buffer + 50 µg/ml chloramphenicol (M9-Cm) followed by M9 buffer, subsequently transferred to individual wells of a 6-well plate filled with sterile M9 buffer + 5 µg/ml cholesterol (M9+Ch Buffer) where they were kept up to 48 hours post exposure (hpe) and imaged after 0, 6 and 30 hpe.

Nematode survival assay

Our goal was to observe infections inside living hosts. To verify that worms stayed alive during the experiment (up to 48 hpe), we tracked the survival of infected population (50-90 worms) in M9-Ch buffer. Worms were observed for motility at 0, 24 and 48 hpe, by prodding them with a platinum wire. Worms were considered dead when they no longer responded to touches. Each bacterial strain was tested in three replicates and three independent experiments were carried out. We used *E. coli* OP50 as a negative control for killing. During this observation period, worms experienced only negligible killing by the colonizing bacteria, and we found no significant difference in killing between the non-pathogenic *E. coli* food strain and the *P. aeruginosa* strains (Supplementary Figure S2).

Microscopy setup and imaging

For microscopy, we picked individual worms from the M9+Ch buffer and paralyzed them with 25 mM sodium azide before transferring them to an 18-well µ-slide (Ibidi, Germany). All experiments were carried out at the Center for Microscope and Image Analysis of the University Zürich (ZMB). For the colonization experiment, images were acquired on a Leica LX inverted widefield light microscope system with Leica-TX2 filter cube for mCherry (emission: 560 ± 40 nm, excitation: 645 ± 75 nm, DM = 595) and Leica-DFC-350-FX, cooled fluorescence monochrome camera (resolution: 1392 × 1040 pixels) for image recording (16-bit color depth). For gene expression experiments, microscopy was performed on the InCell Analyzer 2500HS (GE Healthcare) automated imaging system, using polychroic beam splitter BGRFR_2 (for mCherry, excitation: 575 ± 25 nm, emission: 607.5 ± 19 nm) and PCO – sCMOS camera (resolution: 2048 x 2048 pixels, 16-bit).

Image processing and analysis

To extract fluorescence measurements from individual worms, images were segmented into objects and background, using an automated image segmentation workflow with *ilastik* software [51]. Segmented images were then imported in *Fiji* [52] to determine the fluorescence intensity (as “Raw Integrated Density”, i.e. the sum of pixels values in the selection) and area of each worm. Images obtained from the InCell microscope entailed 64 frames (8x8 grid) with 10% overlap. These frames were stitched together using a macro-automated version of the Stitching plugin in *Fiji* [53] prior to segmentation and analysis. To correct for background and host-tissue autofluorescence, we imaged, at each time point, worms infected with non-

187 fluorescent strains (i.e. OP50 or PAO1), and used the mean intensity of these
188 control infections to subtract background fluorescence values from worms
189 infected with fluorescent strains.
190
191 **Competition assay in the host**
192 For *in-vivo* competitions between PAO1-*mCherry* and PAO1*ΔpvdDΔpchEF* or
193 PAO1*ΔlasR*, overnight monocultures were washed twice with 0.8% NaCl
194 solution, adjusted to OD_{600} = 1 and mixed at a 1:1 ratio. To control for fitness
195 effects of the mCherry marker, we also competed PAO1-*mCherry* against the
196 untagged PAO1. NGM plates were then seeded with 50 µl of mixed culture
197 and incubated at 25°C for 24 hours. Worms were exposed to the mix for 24
198 hours and then recovered as previously described. After 6 and 48 hours post-
199 exposure, individual worms were picked, immobilized with sodium azide and
200 washed for 5 minutes with M9 + 0.003% NaOCl. Worms were washed twice
201 with M9 buffer. We then transferred each individual worm to a 1.5 ml screw-
202 cap micro tube (Sarstedt, Switzerland) containing sterilized glass beads (1 mm
203 diameter, Sigma Aldrich). Worms were disrupted using a bead-beater
204 (TissueLyser II, QIAGEN, Germany), shaking at 30 Hz for 1.5 min before
205 flipping the tubes and shaking for an additional 1.5 min to ensure even
206 disruption (adapted from [54]). Tubes were then centrifuged at 2000 x g for 2
207 min, the content was re-suspended in 200 µl of 0.8% NaCl and plated on two
208 LB 1.2 % agar plates for each sample. Plates were incubated overnight at
209 37°C and left at room temperature for another 24 h to allow the fluorescent
210 marker to fully mature. We then distinguished between fluorescent and non-
211 fluorescent colonies using a custom built fluorescence imaging device (*Infinity*

3 camera, Lumenera, Canada). We then calculated the relative fitness of PAO1-*mCherry* as $\ln(v)=\ln\{[a_{48}\times(1-a_6)]/[a_6\times(1-a_{48})]\}$, where a_6 and a_{48} are the frequency of PAO1-*mCherry* at 6 and 48 hours after recovery, respectively [55]. Values of $\ln(v)<0$ or $\ln(v)>0$ indicate whether the frequency of PAO1-*mCherry* increased ($\ln(v)< 0$) or decreased ($\ln(v)>0$) relative to its competitor.

Co-localization analysis

To determine the degree of co-localization of two different bacterial strains in the host, we transferred nematodes to NGM plates seeded with a 1:1 mix of PAO1-*gfp* with either PAO1-*mCherry*, PAO1*ΔpvdDΔpchEF–mCherry,* or PAO1*ΔlasR-mCherry*. After a 24 hours grazing period, we picked single worms and imaged both mCherry- and GFP channels, using the InCell Analyzer 2500HS microscope. We used *Fiji* to straighten each worm with the *Straighten* plugin [56], and extracted fluorescence intensity values in the GFP and mCherry channels for each pixel from tail (X = 0) to head (X = 1) of the worm. To ensure that we only measure areas where bacteria were present, we restricted our analysis to the region of the worm gut, where bacterial colonization takes place. We then calculated Spearman correlation coefficients between the fluorescent signals, as a proxy for strain co-localization using RStudio v. 3.3.0 [57].

Statistical analysis

All statistical analyses were performed with RStudio. We used Pearson correlations to test for associations between PAO1-*mCherry* fluorescence intensities and (a) recovered bacteria from the gut; and (b) total bacterial load

in mixed infections. We used analysis of variance (ANOVA) to compare fluorescence values between observation times, strains and for comparisons to non-fluorescent controls. *P*-values were corrected for multiple comparisons using the post-hoc Tukey HSD test. To compare promoter expression data between PAO1 WT and mutant strains, and to compare relative fitness values between competitors in the competition assay, we used Welch's two-sample t-test. To measure co-localization, we calculated the Spearman correlation coefficient ρ between the intensity of mCherry and GFP signals across the worm gut, and used ANOVA to test for differences between treatments.

Results

PAO1 colonization dynamics in the *C. elegans* gut

For all infection experiments, we followed the protocol depicted in Figure 1A-C. We first exposed worms to *P. aeruginosa* for 24 hours on NGM plates. Subsequently, worms were removed, washed, and treated with antibiotics to kill external bacteria. We then imaged infected worms under the microscope at different time points and quantified bacterial density and gene expression using fluorescent mCherry markers. We first confirmed that mCherry fluorescence is a suitable proxy for the number of live bacteria in *C. elegans*, by comparing fluorescence intensities in whole worms (Figure 1B) to the number of live bacteria recovered from the worms' gut. Fluorescence intensity values positively correlated with the bacterial load inside the nematodes, both immediately after recovering the worms from the exposure plates and at 6 hours post exposure (hpe; Supplementary Figure S3, Pearson correlation coefficient at 0 hpe: $r = 0.49$, $t_{28} = 3.02$, $p = 0.0053$; at 6 hpe: $r = 0.713$, $t_{23} =$

4.88, $p < 0.0001$). As our goal was to image infections in living hosts, we further confirmed that worms stayed alive during the observation period (Supplementary Figure S2).

When following host colonization by PAO1-*mCherry* over time, we observed that immediately after removal from the exposure plate, worms carried large amounts of bacteria in their gut (Figure 1D). Subsequently, bacterial load significantly declined when worms were kept in buffer for 6 hours (ANOVA: $t_{391} = -8.55$, $p < 0.001$) and then remained constant for the next 24 hours ($t_{391} = 0.61$, $p = 0.529$). This pattern suggests that a large number of bacteria are taken up during the feeding phase, followed by the shedding of a high proportion of cells, leaving behind a fraction of live bacteria that establishes an infection and colonizes the worm gut.

PAO1 expresses siderophore biosynthesis genes and QS regulators in the host

We then examined whether genes involved in the synthesis of pyoverdine (*pvdA*) and pyochelin (*pchEF*), and the genes encoding the QS-regulators *lasR* and *rhlR*, are expressed inside hosts. Worms were exposed to four different PAO1 strains, each carrying a specific promoter-*mCherry* fusion. Imaging after the initial uptake phase (0 hpe) revealed that, with the exception of *pchEF*, all genes were significantly expressed in the host (Figure 2; ANOVA, comparisons to the non-fluorescent control, for *pvdA*: $t_{754} = 4.23$, $p < 0.001$; for *pchEF*: $t_{754} = 0.74$, $p = 0.461$; for *lasR*: $t_{754} = 2.96$, $p = 0.003$; for *rhlR*: $t_{754} = 10.37$, $p < 0.001$). Although fluorescence intensity declined over

time (linear model, $F_{1,1795} = 48.98$, $p < 0.001$), we observed that apart from *pchEF*, all genes were still significantly expressed during the subsequent colonisation of the host at 30 hpe. (Figure 2; ANOVA, for *pvdA*: $t_{754} = 4.87$, $p < 0.001$; for *pchEF*: $t_{754} = 0.684$, $p = 0.461$; for *lasR*: $t_{754} = 3.01$, $p = 0.003$; for *rhlR*: $t_{754} = 16.68$, $p < 0.001$).

Regulatory links between social traits operate inside the host

We know that regulatory links exist between the virulence traits studied here. While pyoverdine synthesis suppresses pyochelin production under stringent iron limitation [58], the Las-QS system positively activates the Rhl-QS system [44]. To test whether these links operate inside the host, we measured gene expression of each trait in the negative background of the co-regulated trait (Figure 3). For *pvdA*, we observed significant gene expression levels in both the wildtype PAO1 and the pyochelin-deficient PAO1Δ*pchEF* strain (Figure 3A), albeit the overall expression was slightly reduced in PAO1Δ*pchEF* (t-test, $t_{253} = 8.67$, $p < 0.001$). For *pchEF*, expression patterns confirm the suppressive nature of pyoverdine: the pyochelin synthesis gene was not expressed in the wildtype but significantly upregulated in the pyoverdine-deficient PAO1Δ*pvdD* strain (Figure 3B; $t_{296} = -19.68$, $p < 0.001$). For *lasR*, we found that gene expression was not significantly different in wildtype PAO1 compared to the Rhl-negative mutant PAO1Δ*rhlR*, confirming that the Las-QS system is at the top of the hierarchy and not influenced by the Rhl-system (Figure 3C; $t_{211} = -1.50$, $p = 0.136$). Conversely, the expression of *rhlR* was strongly dependent on a functional Las-system, and therefore only expressed in PAO1, but repressed in the Las-negative mutant PAO1Δ*lasR* (Figure 3D;

312 t_{156} = 19.04, p < 0.001). These results show that (i) iron-limitation is strong in
313 *C. elegans* as PAO1 primarily invests in the more potent siderophore
314 pyoverdine; (ii) pyochelin can have compensatory effects when pyoverdine is
315 lacking; and (iii) the loss of the Las-system leads to the concomitant collapse
316 of the Rhl-system.
317
318 **Virulence-factor-negative mutants show trait-specific deficiencies in host**
319 **colonization**
320 To examine whether the ability to produce shared virulence factors is
321 important for initial bacterial uptake and host colonization, we exposed
322 *C. elegans* to five isogenic mutants of PAO1-*mCherry*, either impaired in the
323 production of pyoverdine (Δ*pvdD*), pyochelin (Δ*pchEF*), both siderophores
324 (Δ*pvdD*Δ*pchEF*), the QS receptor LasR (Δ*lasR*), or the QS receptor RhlR
325 (Δ*rhlR*). After the feeding phase, the bacterial load of the wildtype and all three
326 siderophores mutants were equally abundant inside hosts, whereas bacterial
327 load was significantly reduced for the two QS-mutants compared to the
328 wildtype (Figure 4A; ANOVA, significant variation among strains $F_{5,736}$ = 10.50,
329 p < 0.001; post-hoc Tukey test for multiple comparisons: p > 0.05 for all
330 siderophore mutants, p = 0.021 for PAO1*ΔlasR*, p < 0.001 for PAO1*ΔrhlR*).
331
332 As previously described for PAO1 colonization (Figure 1D), we observed that
333 the bacterial load of all strains declined at 6 hpe (Supplementary Figure S4)
334 and 30 hpe (Figure 4B) following worm removal from the exposure plates. This
335 decline was significantly more pronounced for the double-siderophore
336 knockout PAO1*ΔpvdDΔpchEF* than for the wildtype (Figure 4B; ANOVA, post-

337 hoc Tukey test $p < 0.001$). In contrast, mutants deficient in pyochelin
338 (PAO1*ΔpchEF*) and RhlR (PAO1*ΔrhlR*) production showed a significantly
339 higher ability to remain in the host than the wildtype (Figure 4B; ANOVA, post-
340 hoc Tukey test $p < 0.001$ for both strains). Taken together, our findings suggest
341 that the two siderophores can complement each other, and that only the
342 siderophore double mutant and the LasR-deficient strain have an overall
343 disadvantage in colonizing worms.
344
345 **Mixed communities are formed inside hosts, but exploitation of social**
346 **traits is constrained**
347 Given our findings on colonization deficiencies, we reasoned that the
348 siderophore-double mutant (PAO1*ΔpvdDΔpchEF*) and the Las-deficient
349 mutant (PAO1*ΔlasR*) could act as cheats and benefit from the exploitation of
350 virulence factors produced by the wildtype in mixed infections. To test this
351 hypothesis, we first competed the PAO1-*mcherry* strain against the untagged
352 wildtype in the host, and found that the mCherry tag had a small negative
353 effect on PAO1 fitness (Figure 5A; one sample t-test, $t_{24} = -4.12$, $p < 0.001$).
354 We then competed PAO1-*mCherry* against the two putative cheats and found
355 that neither of them could gain a significant fitness advantage over the
356 wildtype, but also did not lose out (Figure 5A; ANOVA, $F_{2,70} = 0.517$, $p =$
357 0.598). These results indicate that virulence-factor-negative mutants, initially
358 compromised in host colonization, can indeed benefit from the presence of the
359 wildtype producer, but not to an extent that would allow them to increase in
360 frequency and displace producers.
361

Since our mono-infection experiments showed that the wildtype can maintain higher bacterial loads in the worms compared to the two mutants (Figure 4B), we hypothesized that worms, which have initially taken up higher frequencies of the wildtype relative to the mutant should carry increased bacterial loads in the gut. We found this prediction to hold true at 6 hpe in mixed infections with the two non-producers, but not in the control mixed infections with the untagged wildtype (Figure 5B, 6hpe; Pearson correlation coefficient, for mixed infection with PAO1*ΔlasR*: $r = 0.54$, $t_{17} = 2.67$, $p = 0.016$; with PAO1*ΔpvdDΔpchEF*: $r = 0.40$, $t_{17} = 1.77$, $p = 0.031$; with control PAO1: $r = 0.12$, $t_{17} = 0.47$, $p = 0.639$). These correlations disappeared at the later colonization stage (Figure 5B, 48 hpe; Pearson correlation coefficient $r < 0$, $p > 0.05$ for all strains). The loss of these correlations indicates that rare producers experienced a selective advantage during competition and increased in relative frequency, while common producers might have lost and decreased in frequency.

Strain co-localization is generally high within the host, but varies substantially across individuals

In-vitro studies have shown that spatial proximity of cells is crucial for efficient compound sharing [59, 60]. We thus assessed the co-localization of strains in mixed infections inside the gut (Figure 6). We found that all worms were colonized by both strains, and that the level of co-localization $\boldsymbol{\rho}$ (from tail to head) was generally high, although it varied substantially across individuals (Figure 6A-B). Similar co-localization patterns emerged for all three strain combinations tested, highlighting that the type of competitor did not influence

387 the degree of strain co-localization in the host gut (Figure 6C; ANOVA, $F_{2,102} =$
388 2.17, $p = 0.119$). While our measure of co-localization has some limitations as
389 it does not reveal physical proximity at the single cell level, and is based on a
390 2D projection of a 3D organ, it clearly suggests that competing cells are close
391 to one another, and that social interactions could occur between them.
392
393 **Discussion**
394 We developed a live imaging system that allows us to track host colonization
395 by pathogenic bacteria (*P. aeruginosa*) and their expression of virulence
396 factors inside hosts (*C. elegans*). We used this system to focus on the role of
397 secreted virulence factors, which can be shared as public goods between
398 bacterial cells, and examined competitive dynamics between virulence factor
399 producing and non-producing strains in the host. We found that siderophores
400 (pyoverdine and pyochelin) and the Las and Rhl QS-systems (i) are expressed
401 inside the host; (ii) affect the ability to colonize and reside within the
402 nematodes; (iii) allow non-producers to benefit from virulence factors secreted
403 by producers in mixed infections; but (iv) do not allow non-producers to cheat
404 and outcompete producers. Our results have implications for both the
405 understanding of bacterial social interactions within hosts, and therapeutic
406 approaches that aim to manipulate social dynamics between strains for
407 infection control.
408
409 Numerous *in-vitro* studies have shown that bacterial cooperation can be
410 exploited by cheating mutants that no longer express the social trait, but
411 benefit from the cooperative acts performed by others [3, 11, 12, 55, 61–65].

These findings contrast with our observations that the spread of non-producers was constrained within infections. There are multiple ways to explain this constraint. First, increased spatial structure can limit the diffusion of secreted metabolites and lead to the physical separation of cooperators and cheats [63]. Both effects result in metabolites being shared more locally among cooperative individuals. The physical separation of strains seemed to explain the results of Zhou *et al* [20], where QS-mutants of *Bacillus thuringiensis* infecting caterpillars could not exploit metabolites from producers. Conversely, physical separation seemed low in our study system (Figure 6), and therefore unlikely explains why cheats could not spread. While we solely focussed on proximity patterns inside hosts, it is important to note that processes at the meta-population level such as bottlenecking [54, 66], can reduce the probability of different strains ending up in the same host, and thus further compromise cheat success.

Second, negative frequency-dependent selection could explain why the spread of virulence factor negative mutants is constrained [55]. This scenario predicts that cheats only experience a selective advantage when rare, but not when common. The reasoning is that non-producers can only efficiently exploit public goods when surrounded by many producers. Our competition experiments indeed provide indirect evidence for negative frequency-dependent selection in the nematode gut (Figure 5B). Specifically, we observed that bacterial load was reduced when producers occurred at low frequency early during infection (6 hpe), a result confirming that non-producers are worse host colonizers than producers. These correlations disappeared

437 during the competition period (48 hpe), indicating that rare producers might
438 have experienced a selective advantage and increased in relative frequency,
439 while common producers lost and decreased in frequency.
440
441 Third, the relatively low bacterial density in the gut could further compromise
442 the ability of non-producers to cheat (Figure 1D, 5B). Low cell density restricts
443 the sharing and exploitation of secreted compounds [67, 68]. Mechanisms
444 responsible for the low bacterial density in the gut (Figure 1D, 5B) could
445 include the peristaltic activity of the gut, expelling a part of the pathogen
446 population and the host immune system, killing a fraction of the bacteria [69].
447
448 Fourth, our analysis reveals that, although siderophores and QS-systems play
449 a role in host colonization, they are not essential (Figure 4). Moreover, the
450 expression of pyoverdine and QS-systems declined over time (Figure 2).
451 These two observations indicate that the benefits of cheating might be fairly
452 low, and that the costs of virulence factor production are reduced at later
453 stages of the infection. Thus, bacteria might switch from production to
454 recycling of already secreted public goods [70, 71], an effect that can hamper
455 the spread of cheats.
456
457 Finally, we show that the regulatory linkage between traits is an important
458 factor to consider when predicting the putative advantage of non-producers
459 [72, 73]. For instance, *P. aeruginosa* pyoverdine-negative-mutants
460 upregulated pyochelin production to compensate for the lack of their primary
461 siderophore (Figure 3). Thus, if pyoverdine-negative mutants evolve *de novo*,

462 their spread as cheats could be hampered because they invest in pyochelin as
463 an alternative siderophore [74]. For QS, meanwhile, we observed that the
464 absence of a functional Las-system resulted in the concomitant collapse of the
465 Rhl-system. Although *lasR* mutants could be potent cheats, as they are
466 deficient for multiple social traits, their spread might be hampered because
467 QS-systems also regulate non-social traits, important for individual fitness [75].
468
469 When relating our insights to previous studies, it turns out that earlier work
470 produced mixed results with regard to the question whether siderophore- and
471 QS-deficient mutants can spread within infections. While Harrison *et al*. ([15,
472 21]; pyoverdine, *P. aeruginosa* in *Galleria mellonella* and *ex-vivo* infection
473 models) and Zhou *et al*. ([20]; QS, *B. thuringiensis* in *Plutella xylostella*)
474 showed that the spread of non-producers is constrained, Rumbaugh *et al*.
475 ([16, 17]; QS; *P. aeruginosa* in mice), Pollitt *et al*. ([19]; QS, *Staphylococcus*
476 *aureus* in *G. mellonella*) and Diard *et al*. ([18], T3SS-driven inflammation,
477 *Salmonella typhimorium* in mice) demonstrated cases where non-producers
478 spread to high frequencies in host populations. While the reported results were
479 based on strain frequency counts before and after competition, we here show
480 that information on social trait expression, temporal infection dynamics and
481 physical interactions among strains within hosts are essential to understand
482 whether social traits are important and exploitable in a given system. We thus
483 posit that more such detailed approaches are required to understand the
484 importance of bacterial social interactions across host systems and infection
485 contexts and explain differences between them.
486

A deeper understanding of bacterial social interactions inside hosts is particularly relevant for novel therapeutic approaches that seek to take advantage of cooperator-cheat dynamics inside hosts to control infections. For instance, it was proposed that strains deficient for virulence factors could be introduced into established infections [24]. These strains are expected to spread because of cheating, thereby reducing the overall virulence factor availability in the population and the damage to the host. Our results reveal that virulence-factor-negative strains, although eventually gaining a benefit from producer strains, are unable to spread in populations. Another therapeutic approach involves the specific targeting of secreted virulence factors [25, 27]. This approach is thought to reduce damage to the host and to compromise resistance evolution [30]. Resistant mutants, resuming virulence factor production, are not expected to spread because they would act as cooperators, sharing the benefit of secreted goods with susceptible strains [76–78]. Our results yet indicate that such resistant mutants could get local benefits and thus increase to a certain frequency in the population [31]. These confrontations show that the identification of key parameters driving social interactions across hosts and infection types is of utmost importance to predict the success of ‘cheat therapies’ and anti-virulence strategies targeting secreted public goods.

Acknowledgments

We thank two anonymous reviewers for constructive comments and the Center of Microscopy and Image Analysis (University of Zürich) for support with image acquisition and advice on image analysis.

Funding

This project has received funding from the Swiss National Science Foundation (grant no. PP00P3_165835 and 31003A_182499 to RK and no. P2ZHP3_174751 to EG), and the European Research Council under the grant agreement no. 681295 (to RK).

Competing Interests

The authors have no competing interests to declare.

Supplementary Information

Supplementary information is available at the journal's website.

References:

1. Rahme LG, Stevens EJ, Wolfort SF, Shao J, Tompkins RG, Ausubel FM. Common virulence factors for bacterial pathogenicity in plants and animals. *Science* 1995; **268**: 1899–902.
2. Wu HJ, Wang AHJ, Jennings MP. Discovery of virulence factors of pathogenic bacteria. *Curr Opin Chem Biol* 2008; **12**: 93–101.
3. Diggle SP, Griffin AS, Campbell GS, West SA. Cooperation and conflict in quorum-sensing bacterial populations. *Nature* 2007; **450**: 411–414.
4. Flemming HC, Wingender J, Szewzyk U, Steinberg P, Rice SA, Kjelleberg S. Biofilms: An emergent form of bacterial life. *Nat Rev Microbiol* 2016; **14**: 563–575.
5. Henkel JS, Baldwin MR, Barbieri JT. Toxins from bacteria. *EXS* 2010; **100**: 1–29.
6. Granato ET, Harrison F, Kümmerli R, Ross-Gillespie A. Do Bacterial

"Virulence Factors" Always Increase Virulence? A Meta-Analysis of Pyoverdine Production in *Pseudomonas aeruginosa* As a Test Case. *Front Microbiol* 2016; **7**: 1952.

7. Köhler T, Buckling A, van Delden C. Cooperation and virulence of clinical *Pseudomonas aeruginosa* populations. *Proc Natl Acad Sci USA* 2009; **106**: 6339–6344.

8. Raymond B, West SA, Griffin AS, Bonsall MB. The dynamics of cooperative bacterial virulence in the field. *Science* 2012; **337**: 85–88.

9. Harrison F. Bacterial cooperation in the wild and in the clinic: Are pathogen social behaviours relevant outside the laboratory? *BioEssays* 2013; **35**: 108–112.

10. West SA, Diggle SP, Buckling A, Gardner A, Griffin AS. The Social Lives of Microbes. *Annu Rev Ecol Evol Syst* 2007; **38**: 53–77.

11. Ghoul M, Griffin AS, West SA. Toward an evolutionary definition of cheating. *Evolution* 2014; **68**: 318–331.

12. Özkaya Ö, Balbontín R, Gordo I, Xavier KB. Cheating on Cheaters Stabilizes Cooperation in *Pseudomonas aeruginosa*. *Curr Biol* 2018; **26**: 2070–2080.

13. Buckling A, Brockhurst MA. Kin selection and the evolution of virulence. *Heredity* 2008; **100**: 484–488.

14. Leggett HC, Brown SP, Reece SE. War and peace: social interactions in infections. *Philos Trans R Soc Lond B Biol Sci* 2014; **369**: 20130365.

15. Harrison F, Browning LE, Vos M, Buckling A. Cooperation and virulence in acute *Pseudomonas aeruginosa* infections. *BMC Biol* 2006; **4**: 21.

16. Rumbaugh KP, Diggle SP, Watters CM, Ross-Gillespie A, Griffin AS, West SA. Quorum Sensing and the Social Evolution of Bacterial Virulence. *Curr Biol* 2009; **19**: 341–345.

17. Rumbaugh KP, Trivedi U, Watters C, Burton-Chellew MN, Diggle SP, West SA. Kin selection, quorum sensing and virulence in pathogenic bacteria. *Proc R Soc B Biol Sci* 2012; **279**: 3584–3588.

18. Diard M, Garcia V, Maier L, Remus-Emsermann MNP, Regoes RR, Ackermann M, et al. Stabilization of cooperative virulence by the expression of an avirulent phenotype. *Nature* 2013; **494**: 353–356.

19. Pollitt EJG, West SA, Crusz SA, Burton-Chellew MN, Diggle SP. Cooperation, quorum sensing, and evolution of virulence in *Staphylococcus aureus*. *Infect Immun* 2014; **82**: 1045–1051.

20. Zhou L, Slamti L, Nielsen-LeRoux C, Lereclus D, Raymond B. The Social Biology of Quorum Sensing in a Naturalistic Host Pathogen System. *Curr Biol* 2014; **24**: 2417–2422.

21. Harrison F, McNally A, Da Silva AC, Heeb S, Diggle SP. Optimised chronic infection models demonstrate that siderophore 'cheating' in *Pseudomonas aeruginosa* is context specific. *ISME J* 2017; **11**: 2492–2509.

22. Andersen SB, Marvig RL, Molin S, Krogh Johansen H, Griffin AS. Long-term social dynamics drive loss of function in pathogenic bacteria. *Proc Natl Acad Sci USA* 2015; **112**: 10756–10761.

23. Andersen SB, Ghoul M, Marvig RL, Lee Z Bin, Molin S, Johansen HK, et al. Privatisation rescues function following loss of cooperation. *Elife* 2018; **7**: e38594.

24. Brown SP, West S a, Diggle SP, Griffin AS. Social evolution in micro-organisms and a Trojan horse approach to medical intervention strategies. *Philos Trans R Soc Lond B Biol Sci* 2009; **364**: 3157–3168.

25. Allen RC, Popat R, Diggle SP, Brown SP. Targeting virulence: can we make evolution-proof drugs? *Nat Rev Microbiol* 2014; **12**: 300–308.

26. Granato ET, Ziegenhain C, Marvig RL, Kümmerli R. Low spatial structure and selection against secreted virulence factors attenuates pathogenicity in *Pseudomonas aeruginosa*. *ISME J* 2018; **12**: 2907–2918.

27. André JB, Godelle B. Multicellular organization in bacteria as a target for drug therapy. *Ecol Lett* 2005; **8**: 800–810.

28. Clatworthy AE, Pierson E, Hung DT. Targeting virulence: a new paradigm for antimicrobial therapy. *Nat Chem Biol* 2007; **3**: 541–548.

29. Rasko DA, Sperandio V. Anti-virulence strategies to combat bacteria-mediated disease. *Nat Rev Drug Discov* 2010; **9**: 117–128.

30. Pepper JW. Drugs that target pathogen public goods are robust against evolved drug resistance. *Evol Appl* 2012; **5**: 757–761.

31. Rezzoagli C, Wilson D, Weigert M, Wyder S, Kümmerli R. Probing the evolutionary robustness of two repurposed drugs targeting iron uptake in *Pseudomonas aeruginosa*. *Evol Med Public Heal* 2018; **1**: 246–259.

32. Tan MW, Ausubel FM. *Caenorhabditis elegans*: A model genetic host to study *Pseudomonas aeruginosa* pathogenesis. *Curr Opin Microbiol* 2000; **3**: 29–34.

33. Ewbank JJ. Tackling both sides of the host – pathogen equation with *Caenorhabditis elegans*. *Microbes Infect* 2002; **4**: 247–256.

34. Papaioannou E, Utari P, Quax W. Choosing an Appropriate Infection Model to Study Quorum Sensing Inhibition in *Pseudomonas Infections*. *Int J Mol Sci* 2013; **14**: 19309–19340.

35. Félix M-A, Braendle C. The natural history of *Caenorhabditis elegans*. *Curr Biol* 2010; **20**: R965–R969.

36. Portal-Celhay C, Bradley ER, Blaser MJ. Control of intestinal bacterial proliferation in regulation of lifespan in *Caenorhabditis elegans*. *BMC Microbiol* 2012; **12**: 49.

37. Tan MW, Mahajan-Miklos S, Ausubel FM. Killing of *Caenorhabditis elegans* by *Pseudomonas aeruginosa* used to model mammalian bacterial pathogenesis. *Proc Natl Acad Sci USA* 1999; **96**: 715–20.

38. Jimenez PN, Koch G, Thompson JA, Xavier KB, Cool RH, Quax WJ. The multiple signaling systems regulating virulence in *Pseudomonas aeruginosa*. *Microbiol Mol Biol Rev* 2012; **76**: 46–65.

39. Meyer JM, Neely A, Stintzi A, Georges C, Holder IA. Pyoverdin is essential for virulence of *Pseudomonas aeruginosa*. *Infect Immun* 1996;

64: 518–523.

40. Takase H, Nitanai H, Hoshino K, Otani T. Impact of Siderophore Production on *Pseudomonas aeruginosa* Infections in Immunosuppressed Mice. *Infect Immun* 2000; **68**: 1834–1839.

41. Cornelis P, Dingemans J. *Pseudomonas aeruginosa* adapts its iron uptake strategies in function of the type of infections. *Front Cell Infect Microbiol* 2013; **3**: 1–7.

42. Smith RS, Iglewski BH. *P. aeruginosa* quorum-sensing systems and virulence. *Curr Opin Microbiol* 2003; **6**: 56–60.

43. Alibaud L, Köhler T, Coudray A, Prigent-Combaret C, Bergeret E, Perrin J, et al. *Pseudomonas aeruginosa* virulence genes identified in a *Dictyostelium* host model. *Cell Microbiol* 2008; **10**: 729–740.

44. Lee J, Zhang L. The hierarchy quorum sensing network in Pseudomonas aeruginosa. *Protein Cell* 2015; **6**: 26–41.

45. Zaborin A, Romanowski K, Gerdes S, Holbrook C, Lepine F, Long J, et al. Red death in *Caenorhabditis elegans* caused by *Pseudomonas aeruginosa* PAO1. *Proc Natl Acad Sci USA* 2009; **106**: 6327–32.

46. Kirienko N V., Kirienko DR, Larkins-Ford J, W??hlby C, Ruvkun G, Ausubel FM. Pseudomonas aeruginosa disrupts Caenorhabditis elegans iron homeostasis, causing a hypoxic response and death. *Cell Host Microbe* 2013; **13**: 406–416.

47. Cezairliyan B, Vinayavekhin N, Grenfell-Lee D, Yuen GJ, Saghatelian A, Ausubel FM. Identification of *Pseudomonas aeruginosa* phenazines that kill *Caenorhabditis elegans*. *PLOS Pathog* 2013; **9**: e1003101.

48. Zhu J, Cai X, Harris TL, Gooyit M, Wood M, Lardy M, et al. Disarming *Pseudomonas aeruginosa* Virulence Factor LasB by Leveraging a *Caenorhabditis elegans* Infection Model. *Chem Biol* 2015; **22**: 483–491.

49. Stiernagle T. Maintenance of C. elegans. In: The *C.elegans* Research Community (ed). *WormBook: The Online Review of C. elegans Biology.* 2006.

50. Portman DS. Profiling C. elegans gene expression with DNA microarrays. In: The C.elegans Research Community (ed). *WormBook: The Online Review of C. elegans Biology.* 2006.

51. Sommer C, Strähle C, Köthe U, Hamprecht FA. ilastik: Interactive Learning and Segmentation Toolkit. *Eighth IEEE Int. Symp. Biomed. Imaging (ISBI). Proc.* 2011. pp 230–233.

52. Schindelin J, Arganda-Carreras I, Frise E, Kaynig V, Longair M, Pietzsch T, et al. Fiji: an open-source platform for biological-image analysis. *Nat Methods* 2012; **9**: 676–82.

53. Preibisch S, Saalfeld S, Tomancak P. Globally optimal stitching of tiled 3D microscopic image acquisitions. *Bioinformatics* 2009; **25**: 1463–1465.

54. Vega NM, Gore J. Stochastic assembly produces heterogeneous communities in the *Caenorhabditis elegans* intestine. *PLOS Biol* 2017; **15**: e2000633.

55. Ross-Gillespie A, Gardner A, West SA, Griffin AS. Frequency dependence and cooperation: theory and a test with bacteria. *Am Nat* 2007; **170**: 331–342.

56. Kocsis E, Trus BL, Steer CJ, Bisher ME, Steven AC. Image averaging of flexible fibrous macromolecules: the clathrin triskelion has an elastic proximal segment. *J Struct Biol* 1991; **107**: 6–14.

57. R Development Core Team. R: A language and environment for statistical computing. *R Foundation for Statistical Computing*. 2013. Vienna, Austria.

58. Dumas Z, Ross-Gillespie A, Kümmerli R. Switching between apparently redundant iron-uptake mechanisms benefits bacteria in changeable environments. *Proc Biol Sci* 2013; **280**: 20131055.

59. Van Gestel J, Weissing FJ, Kuipers OP, Kovács ÁT. Density of founder cells affects spatial pattern formation and cooperation in *Bacillus subtilis* biofilms. *ISME J* 2014; **8**: 2069–2079.

689 60. Weigert M, Kümmerli R. The physical boundaries of public goods
690 cooperation between surface-attached bacterial cells. *Proc R Soc B Biol*
691 *Sci* 2017; **284**: 20170631.

692 61. Griffin AS, West SA, Buckling A. Cooperation and competition in
693 pathogenic bacteria. *Nature* 2004; **430**: 1024–1027.

694 62. Sandoz KM, Mitzimberg SM, Schuster M. Social cheating in
695 *Pseudomonas aeruginosa* quorum sensing. *Proc Natl Acad Sci USA*
696 2007; **104**: 15876–81.

697 63. Kümmerli R, Griffin AS, West S a, Buckling A, Harrison F. Viscous
698 medium promotes cooperation in the pathogenic bacterium
699 *Pseudomonas aeruginosa*. *Proc Biol Sci* 2009; **276**: 3531–3538.

700 64. Popat R, Crusz SA, Messina M, Williams P, West SA, Diggle SP.
701 Quorum-sensing and cheating in bacterial biofilms. *Proc R Soc B Biol*
702 *Sci* 2012; **279**: 4765–4771.

703 65. O'Brien S, Luján AM, Paterson S, Cant MA, Buckling A. Adaptation to
704 public goods cheats in *Pseudomonas aeruginosa*. *Proc R Soc B Biol Sci*
705 2017; **284**: 20171089.

706 66. van Leeuwen E, O'Neill S, Matthews A, Raymond B. Making pathogens
707 sociable: The emergence of high relatedness through limited host
708 invasibility. *ISME J* 2015; **9**: 2315–2323.

709 67. Ross-Gillespie A, Gardner A, Buckling A, West SA, Griffin AS. Density
710 dependence and cooperation: theory and a test with bacteria. *Evolution*
711 2009; **63**: 2315–2325.

712 68. Scholz RL, Greenberg EP. Sociality in *Escherichia coli*: Enterochelin Is a
713 Private Good at Low Cell Density and Can Be Shared at High Cell
714 Density. *J Bacteriol* 2015; **197**: 2122–2128.

715 69. Pukkila-Worley R, Ausubel FM. Immune defense mechanisms in the
716 *Caenorhabditis elegans* intestinal epithelium. *Curr Opin Immunol* 2012;
717 **24**: 3–9.

718 70. Imperi F, Tiburzi F, Visca P. Molecular basis of pyoverdine siderophore

recycling in *Pseudomonas aeruginosa*. *Proc Natl Acad Sci USA* 2009; **106**: 20440–20445.

71. Kümmerli R, Brown SP. Molecular and regulatory properties of a public good shape the evolution of cooperation. *Proc Natl Acad Sci USA* 2010; **107**: 18921–6.

72. Lindsay RJ, Kershaw MJ, Pawlowska BJ, Talbot NJ, Gudelj I. Harbouring public good mutants within a pathogen population can increase both fitness and virulence. *Elife* 2016; **5**: 1–25.

73. dos Santos M, Ghoul M, West SA. Pleiotropy, cooperation and the social evolution of genetic architecture. *PLOS Biol* 2018; **16**: e2006671.

74. Ross-Gillespie A, Dumas Z, Kümmerli R. Evolutionary dynamics of interlinked public goods traits: An experimental study of siderophore production in *Pseudomonas aeruginosa*. *J Evol Biol* 2015; **28**: 29–39.

75. Dandekar AA, Chugani S, Greenberg PE. Bacterial Quorum Sensing and Metabolic Incentives to Cooperate. *Science* 2012; **338**: 264–266.

76. Mellbye B, Schuster M. The sociomicrobiology of antivirulence drug resistance: a proof of concept. *MBio* 2011; **2**: e00131-11.

77. Gerdt JP, Blackwell HE. Competition Studies Confirm Two Major Barriers That Can Preclude the Spread of Resistance to Quorum-Sensing Inhibitors in Bacteria. *ACS Chem Biol* 2014; **9**: 2291–2299.

78. Ross-Gillespie A, Weigert M, Brown SP, Kümmerli R. Gallium-mediated siderophore quenching as an evolutionarily robust antibacterial treatment. *Evol Med Public Heal* 2014; **2014**: 18–29.

Figure captions

Figure 1. Quantifying *P. aeruginosa* infections in the *C. elegans* gut. (A) Experimental procedure: we used fluorescently tagged *P. aeruginosa* strains to examine bacterial colonization of the *C. elegans* gut. Per experiment, we exposed approximately 200 *C. elegans* nematodes to a lawn of mCherry-tagged PAO1 strains for 24 hours. Subsequently, nematodes were removed from the bacterial plate, surface washed and collected in sterile buffer for monitoring. After 0, 6, or 30 hours post exposure (hpe), approximately 30 nematodes were immobilized and transferred to microscopy slides for imaging. (B) Brightfield and fluorescence channel merged image depicting mCherry-fluorescent bacteria inside the host gut. (C) Bacterial load inside the nematode was quantified as the sum of fluorescence intensity across pixels in the region of interest "ROI" (yellow outline) and standardised by total worm area. (D) Colonization dynamics of the wildtype strain PAO1-*mCherry*: immediately after removal from the exposure plate (0 hpe), worms showed high bacterial loads inside their guts. Bacterial load first declined when the worms where kept in buffer for 6 hours, but then remained constant for the next 24 hours. Grey shaded area indicates background fluorescence (mean +/- standard deviation) of worms exposed to the non-fluorescent, non-pathogenic *E.coli* OP50. N = number of worms from four independent experiments. *** = $p < 0.001$, n.s. = not statistically significant.

Figure 2. *P. aeruginosa* expresses genes for pyoverdine synthesis and quorum sensing regulators in the host gut. To quantify the expression of virulence factor genes inside hosts, worms were exposed to four PAO1

768 strains, each containing a promoter::*mCherry* fusion for either *pvdA*
769 *(*pyoverdine synthesis*), pchEF* (pyochelin synthesis), *lasR* or *rhlR* (quorum
770 sensing regulators). With the exception of *pchEF*, all genes were significantly
771 expressed in the host, both at 0 and 30 hpe. Expression levels were
772 standardised for bacterial load. Grey shaded areas depict background
773 fluorescence (mean +/- standard deviation) of worms exposed to the non-
774 fluorescent, non-pathogenic *E.coli* OP50. N = number of worms from four
775 independent experiments. * = $p < 0.05$; ** = $p < 0.01$, *** = $p < 0.001$, n.s. = not
776 statistically significant.
777
778 **Figure 3. *P. aeruginosa* can switch between siderophores, while quorum**
779 **sensing regulators act hierarchically.** Because virulence traits are linked at
780 the regulatory level, we measured gene expression of each trait in the
781 negative background of the co-regulated trait. (A) The expression of the
782 pyoverdine synthetic gene *pvdA* is significantly expressed in the wildtype and
783 the pyochelin-negative background, but slightly reduced in the latter. (B) The
784 pyochelin synthetic gene *pchEF* is significantly expressed in the pyoverdine-
785 negative background, but silent in the wildtype. (C) The expression of the QS-
786 regulator gene *lasR* is unchanged in the Rhl-negative background compared
787 to the wildtype. (D) The expression of the QS-regulator gene *rhlR* is reduced in
788 the Las-negative background. Expression levels were standardised for
789 bacterial load. Grey shaded areas depict background fluorescence (mean +/-
790 standard deviation) of worms exposed to the non-fluorescent, non-pathogenic
791 *E.coli* OP50. N = number of worms form four independent experiments. * = $p <$
792 0.05; ** = $p < 0.01$, *** = $p < 0.001$, n.s. = not statistically significant.

Figure 4. Virulence factor production affects bacterial uptake and host colonization ability. (A) Bacterial load inside *C. elegans* guts measured immediately after the recovery of worms from the exposure plates (0 hours post exposure; hpe). Comparisons across isogenic PAO1 mutant strains, each deficient for the production of one or two virulence factors, reveal that the two quorum-sensing mutants PAO1Δ*lasR* and PAO1Δ*rhlR* reached lower bacterial densities than the wildtype. (B) Comparison of the relative colonization success of strains (ratio of bacterial loads at 0 hpe versus 30 hpe) revealed that the siderophore-negative strain PAO1*ΔpvdDΔpchEF* showed significantly reduced ability to remain in the host compared to the wildtype. In contrast, the colonisation success of PAO1Δ*pchEF* and PAO1Δ*rhlR* was increased relative to the wildtype. Grey shaded areas depict background fluorescence (mean +/- standard deviation) of worms exposed to the non-fluorescent, non-pathogenic *E.coli* OP50. N = number of worms form four independent experiments. * = $p < 0.05$; ** = $p < 0.01$, *** = $p < 0.001$.

Figure 5. Mixed infections reveal social strain dynamics but no successful cheating. (A) Relative fitness of the wildtype PAO1-*mCherry* after 42 hours of competition inside the *C. elegans* gut against an untagged PAO1 control strain; the siderophore-negative strain PAO1Δ*pvdDΔpchEF*; and the Las-negative strain PAO1Δ*lasR*. The control competition revealed a mild but significant negative effect of the mCherry tag on wildtype fitness. When accounting for these mCherry costs, we found that the putative cheat strains PAO1 Δ*lasR* and PAO1 Δ*pvdDΔpchEF* performed equally well compared to

818 the wildtype, but could not outcompete it. This suggests that virulence factor
819 deficient strains benefit from the presence of non-producers but cannot
820 successfully cheat on them. (B) At 6 hpe, wildtype frequency in mixed
821 infections correlated positively with total bacterial load inside hosts in
822 competition with PAO1Δ*lasR* (squares and dashed lines) and
823 PAO1Δ*pvdD*Δ*pchEF* (diamonds and dotted lines) but not in the control
824 competition (circles and solid lines). These correlations disappeared at 48 hpe.
825 Each data point represents an individual worm. Data shown in A+B stem from
826 the same three independent experiments.
827
828 **Figure 6. Spatial structure of mixed infections in the nematode gut.** (A, B)
829 Illustrative examples of *C. elegans* individuals infected with a mixture of GFP-
830 and mCherry-labelled strains. Each worm was computationally straightened
831 and fluorescence intensity values were extracted for each pixel from tail (X=0)
832 to head (X=1). We then calculated the Spearman correlation coefficient ρ
833 between the intensity values in the two fluorescence channels across pixels,
834 as our estimate of strain colocalization. Examples show worms with high (A)
835 and low (B) degrees of colocalization. (C) Patterns of colocalization levels
836 varied substantially between individuals, but did not differ across strain
837 combinations ($p = 0.119$: wildtype PAO1-*mCherry* versus: (i) wildtype PAO1-
838 *gfp* (circles), (ii) PAO1Δ*pvdD*Δ*pchEF-mCherry* (diamonds) or (iii) PAO1Δ*lasR*-
839 *mCherry* (squares). Each data point represents an individual worm. Data
840 stems from 3 independent experiments, with 12 replicates each.

A

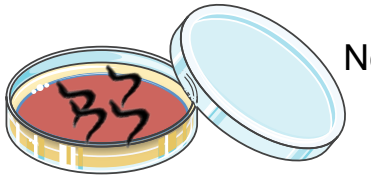

Nematodes washed with buffer + antibiotic

0 hpe

6 hpe

30 hpe

Nematodes immobilized (25 mM NaN_3)

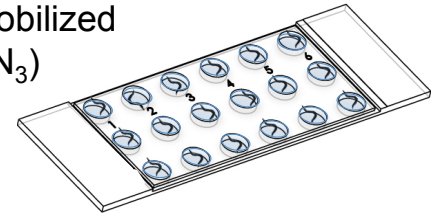

Exposure

Host exposed to mCherry-tagged *P. aeruginosa* strains for 24 h

Observation and measurements

Removal from exposure plate, collection in sterile buffer and microscopy measurement taken at 0, 6 and 30 hours post exposure (hpe).

B

C

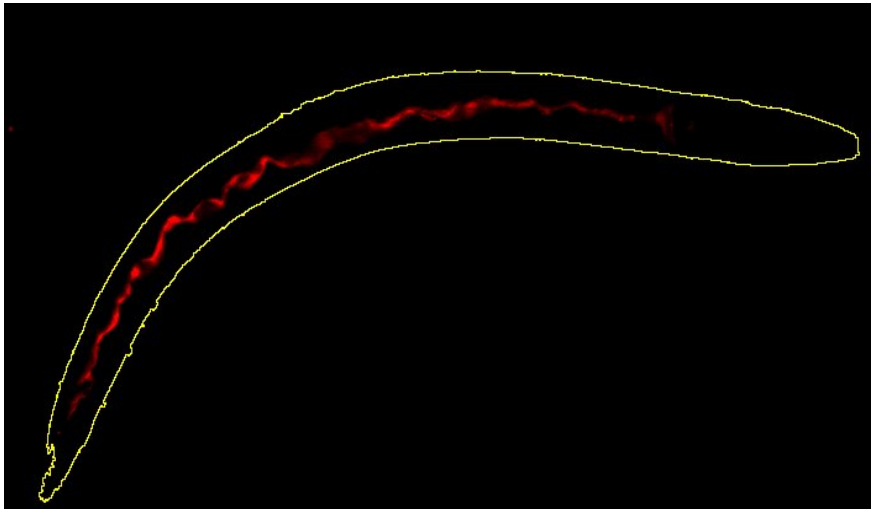

D

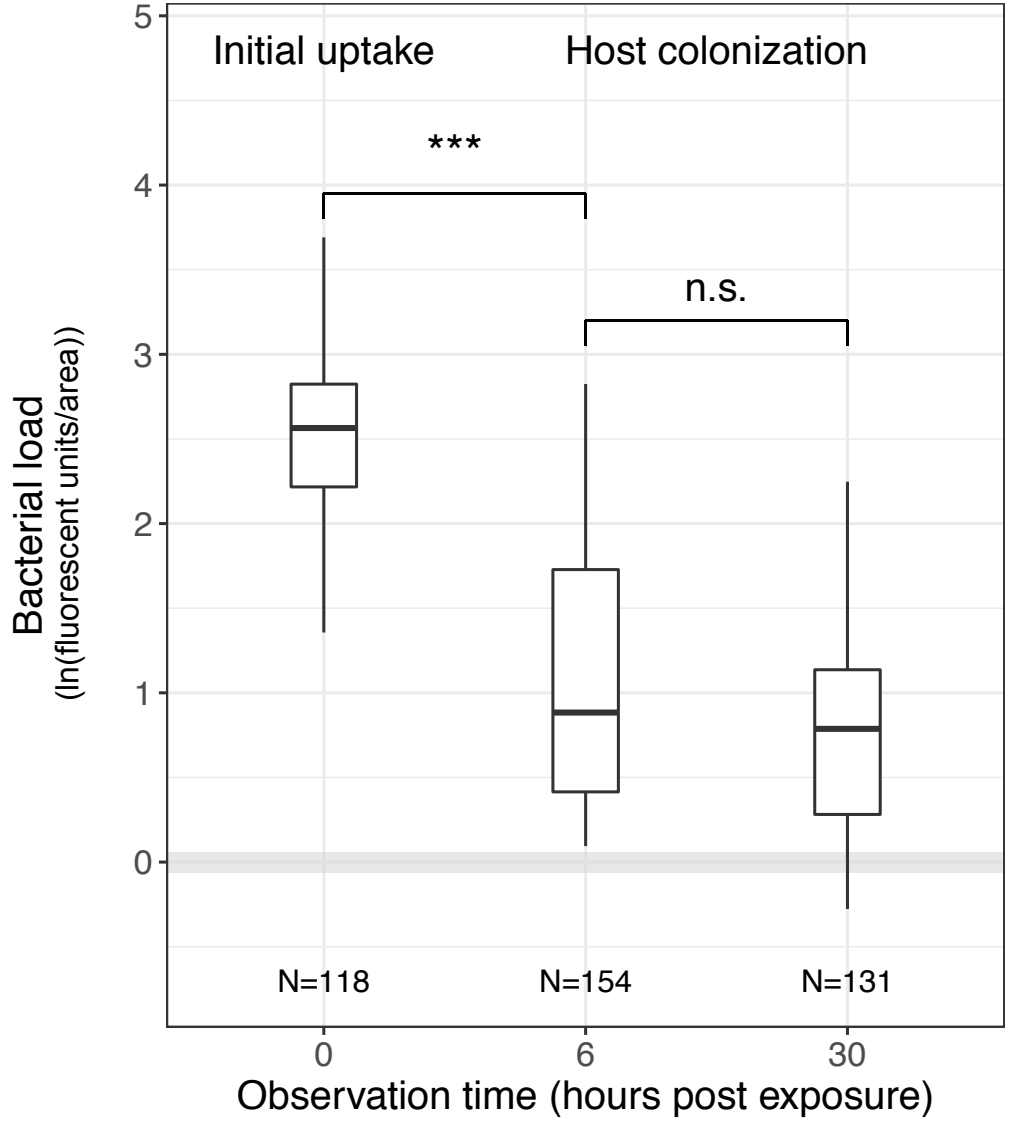

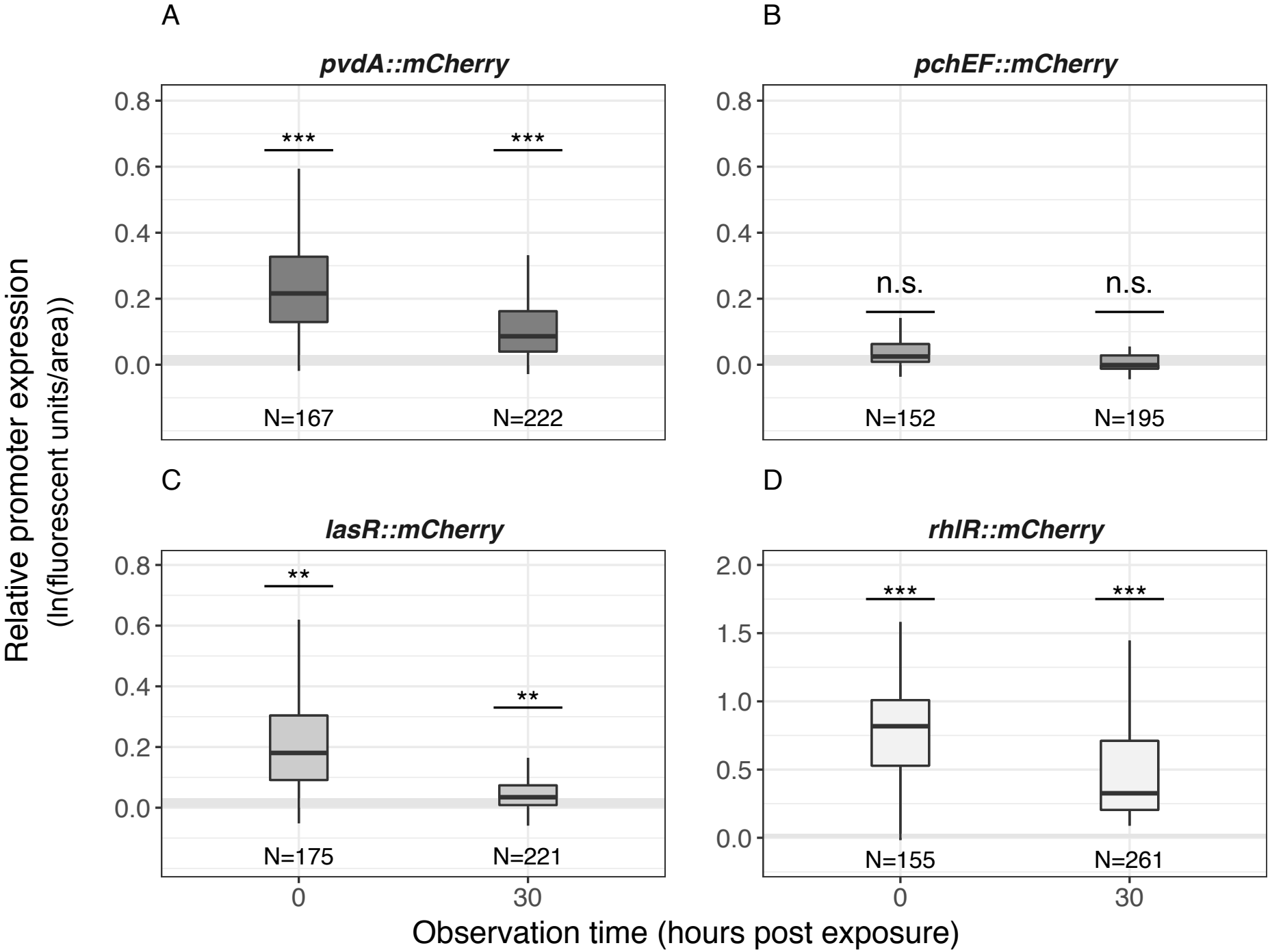
A
pvdA::mCherry
B
pchEF::mCherry
C
lasR::mCherry
D
rhlR::mCherry
Relative promoter expression
(ln(fluorescent units/area))
0.8
0.6
0.4
0.2
0.0
2.0
1.5
1.0
0.5
***
**
n.s.
N=167
N=222
N=152
N=195
N=175
N=221
N=155
N=261
0
30
Observation time (hours post exposure)

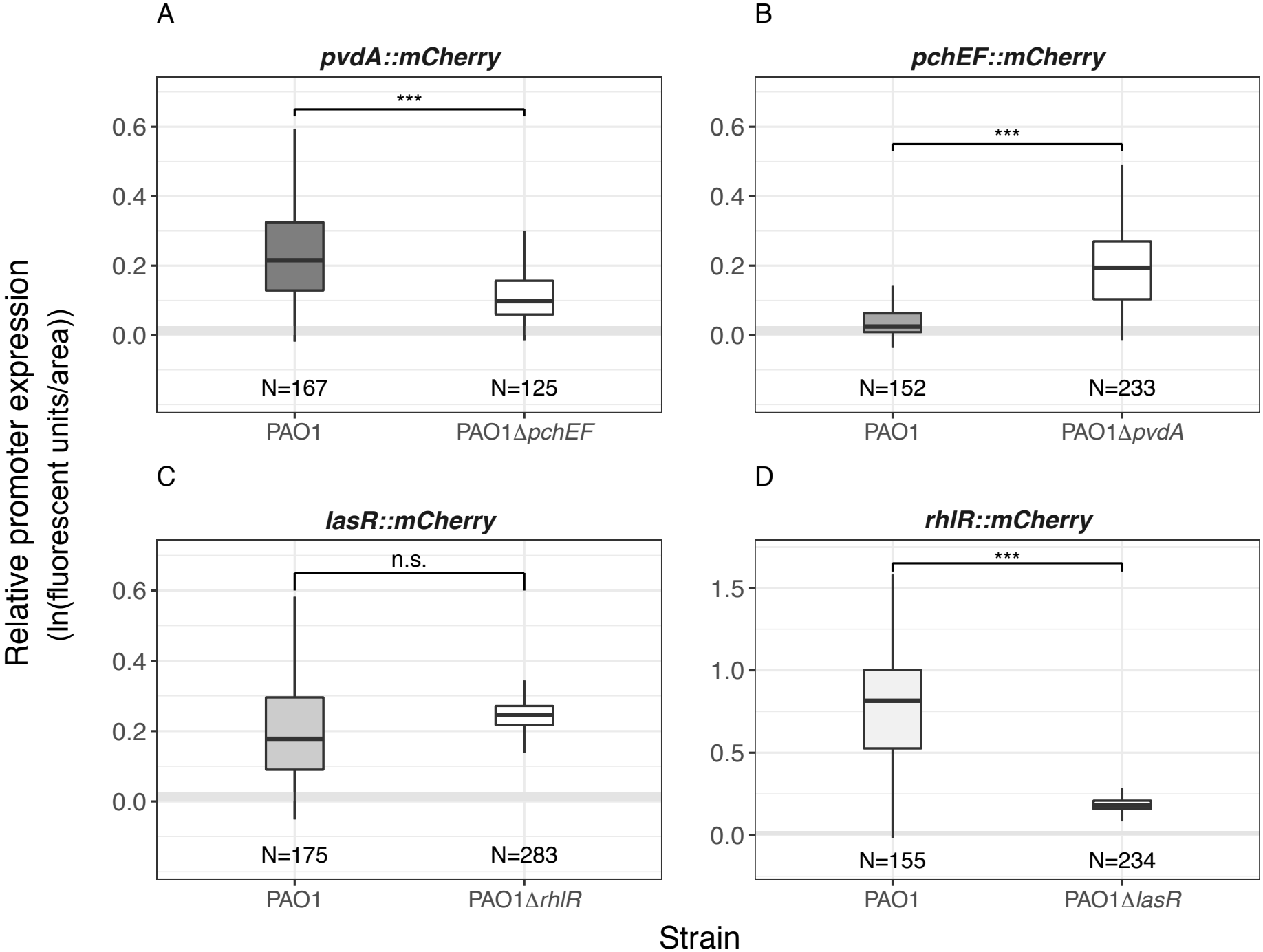
A
pvdA::mCherry
***
0.6
0.4
0.2
0.0
N=167
N=125
PAO1
PAO1ΔpchEF
B
pchEF::mCherry
***
0.6
0.4
0.2
0.0
N=152
N=233
PAO1
PAO1ΔpvdA
C
lasR::mCherry
n.s.
0.6
0.4
0.2
0.0
N=175
N=283
PAO1
PAO1ΔrhlR
D
rhlR::mCherry
***
1.5
1.0
0.5
0.0
N=155
N=234
PAO1
PAO1ΔlasR
Relative promoter expression
(ln(fluorescent units/area))
Strain

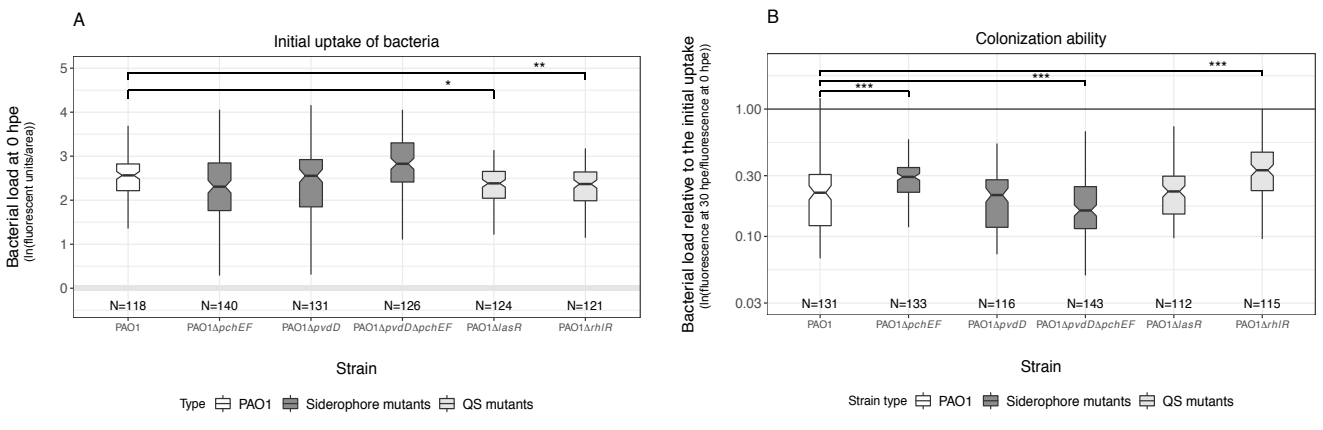
A
Initial uptake of bacteria
Bacterial load at 0 hpe
(ln(fluorescent units/area))
5
4
3
2
1
0
**
*
N=118
N=140
N=131
N=126
N=124
N=121
PAO1
PAO1ΔpchEF
PAO1ΔpvdD
PAO1ΔpvdDΔpchEF
PAO1ΔlasR
PAO1ΔrhlR
Strain
Type PAO1 Siderophore mutants QS mutants
B
Colonization ability
Bacterial load relative to the initial uptake
(ln(fluorescence at 30 hpe/fluorescence at 0 hpe))
1.00
0.30
0.10
0.03
***
***
***
N=131
N=133
N=116
N=143
N=112
N=115
PAO1
PAO1ΔpchEF
PAO1ΔpvdD
PAO1ΔpvdDΔpchEF
PAO1ΔlasR
PAO1ΔrhlR
Strain
Strain type PAO1 Siderophore mutants QS mutants

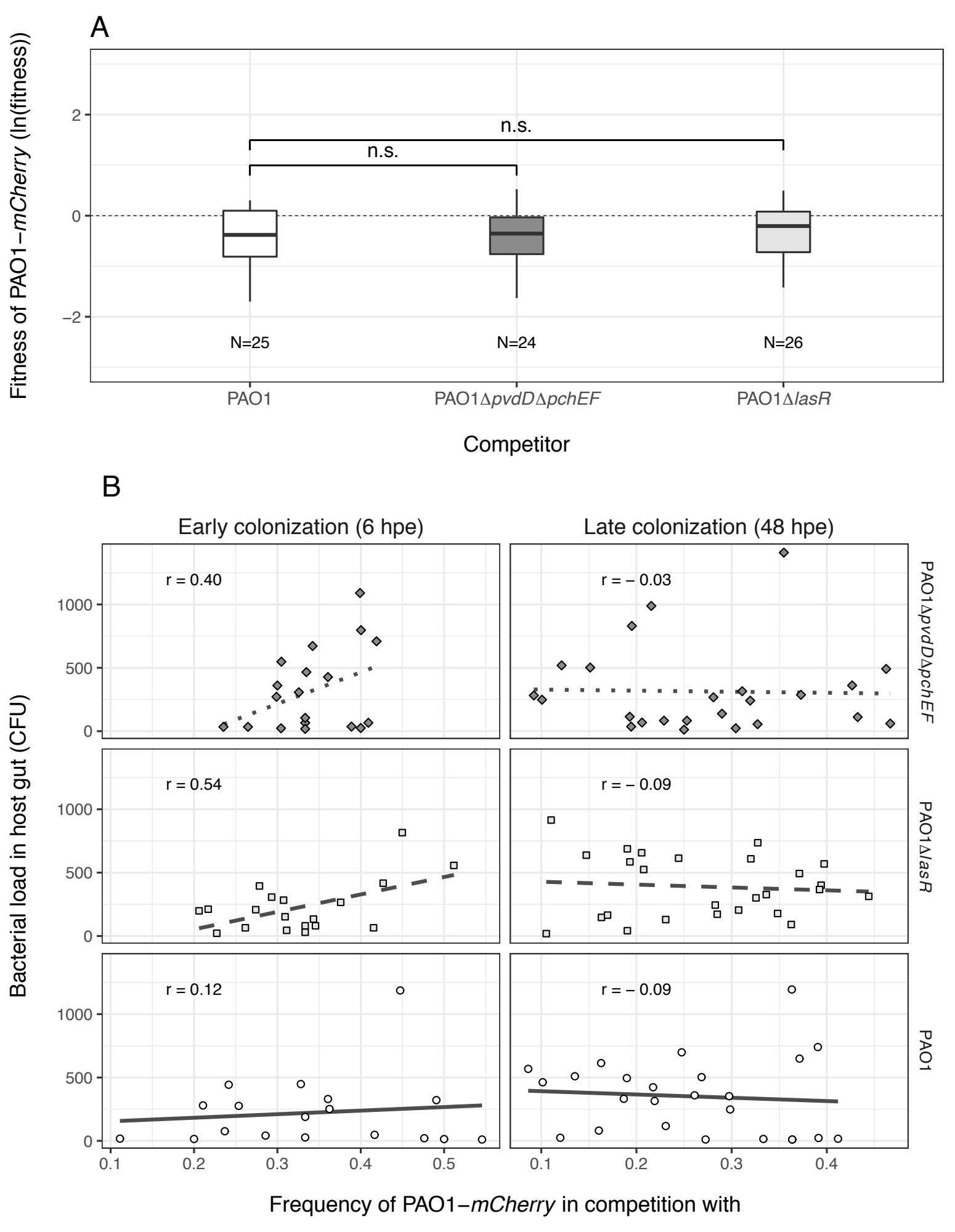
A
Fitness of PAO1–mCherry (ln(fitness))
2
0
−2
n.s.
n.s.
N=25
N=24
N=26
PAO1
PAO1ΔpvdDΔpchEF
PAO1ΔlasR
Competitor
B
Early colonization (6 hpe)
Late colonization (48 hpe)
Bacterial load in host gut (CFU)
r = 0.40
r = – 0.03
r = 0.54
r = – 0.09
r = 0.12
r = – 0.09
PAO1ΔpvdDΔpchEF
PAO1ΔlasR
PAO1
1000
500
0
0.1
0.2
0.3
0.4
0.5
Frequency of PAO1–mCherry in competition with

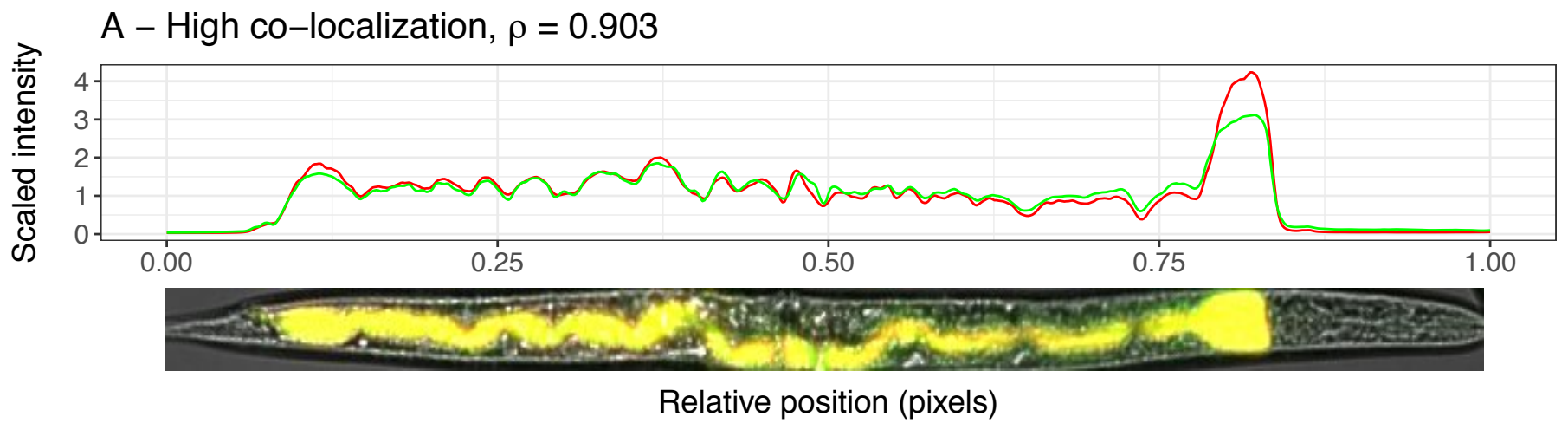
A – High co–localization, ρ = 0.903
Scaled intensity
4
3
2
1
0
0.00
0.25
0.50
0.75
1.00
Relative position (pixels)

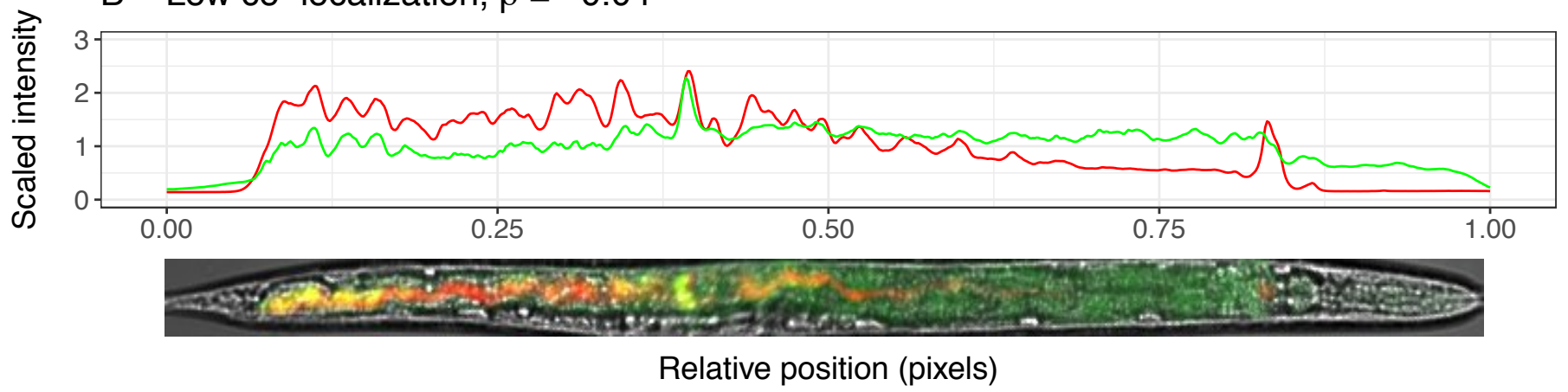
B – Low co–localization, ρ = −0.04
Scaled intensity
3
2
1
0
0.00
0.25
0.50
0.75
1.00
Relative position (pixels)

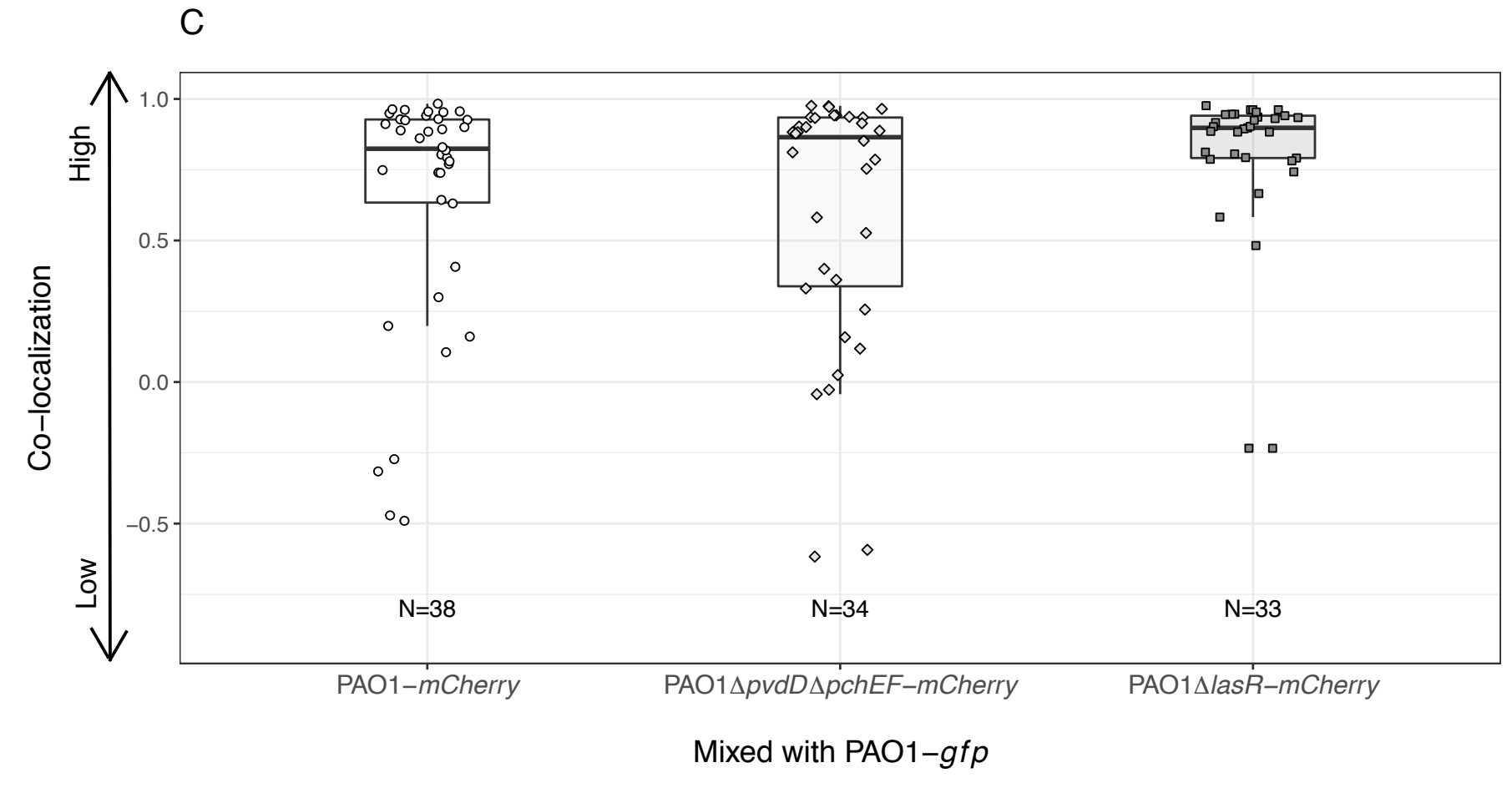
C
Co–localization
High
Low
1.0
0.5
0.0
−0.5
N=38
N=34
N=33
PAO1–mCherry
PAO1ΔpvdDΔpchEF–mCherry
PAO1ΔlasR–mCherry
Mixed with PAO1–gfp